

# TVA tungsten plasma parameters for hard coatings

C. Porosnicu<sup>1</sup>, M. Osiac<sup>2</sup>, E. Osiac<sup>3</sup>, C. P. Lungu<sup>1</sup>

<sup>1</sup>National Institute for Laser, Plasma and Radiation Physics,  
Magurele, 077125, Romania

<sup>2</sup>Faculty of Physics, University of Craiova, Craiova, 200585, Romania  
e-mail: m\_osiac@yahoo.com

<sup>3</sup>Univ Med & Pharm Craiova, Craiova 1100, Romania

## Abstract

The paper presents a tungsten layer deposited on a stainless steel surface by thermionic vacuum arc (TVA) plasma. The deposition is obtained during stable TVA arc plasma conditions. The temperature of the top of wolfram anode, the evaporation rate and the metallic pressure were measured. A X ray diffraction (XRD) and atomic force microscopy (AFM) were used for analyzing the film structure and the surface roughness.

## 1 Introduction

Hard coatings deposition has been considered an excellent way to increase the life of tools by improving their resistance to corrosion, oxidation and wear. Many industrial tools are exposed to severe working conditions, such as, high temperatures and oxidizing atmospheres. In general, coatings designed to provide high temperatures oxidation resistance can form a protective oxide film on surface, which can protect the coating from further attack by reactive gas. A controlled oxidation process is necessary to use the benefits of a thin adherent oxide film [1]. In general, the tungsten layers either tungsten oxide layer were obtained using a magnetron sputtering discharge [2], the electron beam deposition technique [3] and chemical vapor deposition that uses a tungsten hexaphenoxide [4].

In the present paper the tungsten layer was obtained by TVA method. The TVA plasma has many advantages over the known plasma deposition techniques as pulsed laser deposition, magnetron sputtering, chemical vapor deposition, etc. An important advantage of the TVA method is specific to application of high-temperature resistant films. In this method no gas precursors or carrier gases is needed, so no gas inclusions is present in the obtained films. The TVA was proved to be the excellent method in deposition of films of high melting temperature materials such as rhenium, nickel, chromium [5]. The refractory materials (Re, W, Ni, Cr) are difficult to process due to the fact that no crucible material can resist the high temperature necessary for their melting and evaporation. Thus the TVA is unique since a crucible is not needed to provide the vapors required for igniting corresponding plasma. This is due to the fact that the TVA is ignited locally,

above the anode, in the vapors of the material, at vapor pressures of few Torr. Such vapor pressures can be obtained just by heating the surface of the material/metal without melting the whole anode rod: an electron beam generated by a heated filament is utilized for this purpose. The metal vapors are then ionized by fast electrons accelerated by the anode. Under certain operating electrical parameters, the plasma becomes stable and can be maintained longer if the anode material is present. In the present paper a tungsten layer was deposited on a stainless steel surface during TVA stable conditions. The anode temperature, vapor pressure and speed evaporation were measured. The tungsten film structure was obtained by XRD measurements and the layer roughness was measured by AFM.

## 2 Experimental Section

The experimental set-up is presented elsewhere [6] and briefly consists of a tungsten filament cathode externally heated by a low voltage and a tungsten rod anode. The thermal electrons emitted are focused on the top of the anode surface by a Wienelt cylinder. The anode is a  $8mm$  diameter and  $80mm$  long tungsten rod on which positive high voltage is applied. Due to electron bombardment, the anode material evaporates and at a certain vapor pressure the electron-atom ionizing collisions generate a plasma in pure anode material. The substrates to be deposited were placed  $200 - 250mm$  away above the anode. Stainless steel was used as substrates. For estimation of anode temperature, the thermal radiation of the top anode was recorded using a SM-240 CCD Optical Multichannel Analyzer. The thermal radiation was focused by a convergent lens on the entrance slit of the spectrograph. A  $2mm$  diameter iris diaphragm was used to take the light from a small region of the anode. The schematic experimental set-up is presented in Figure 1.

## 3 Results and Discussion

Emission spectra of the tungsten TVA plasma as well as the thermal radiation of the top anode were acquired during plasma ignition. System calibration was undertaken using a ribbon tungsten lamp. The anode temperature during plasma ignition was calculated using the Stefan-Boltzmann relation (1) and the thermal radiation spectrum,

$$A = \sigma \varepsilon T^4 \quad (1)$$

where  $A$  is the area under the thermal radiation curve,  $\sigma$  is the Boltzmann constant,  $\varepsilon$  is the emissivity of tungsten in the  $300 - 800nm$  spectral region [7], quite close to the melting point and  $T$  is the top anode temperature. An important error factor in the measurements of tungsten anode temperature is deposition on the aimer window.

In Figure 2 is shown the top anode temperature during the arc discharge for two filament currents. It could be observed that during the plasma deposition the anode temperatures are quite high and has constant values.

The errors in Figure 2 were estimated to be 10%. In general, in the TVA plasma, it was found that the anode temperature increased proportionally with increasing power until the moment of plasma ignition, at around melting temperature of the anode material [8]. The temperature had an almost constant value during arc ignition even for higher power input which suggests that a balance between tungsten atoms evaporation and plasma ionization is reached.

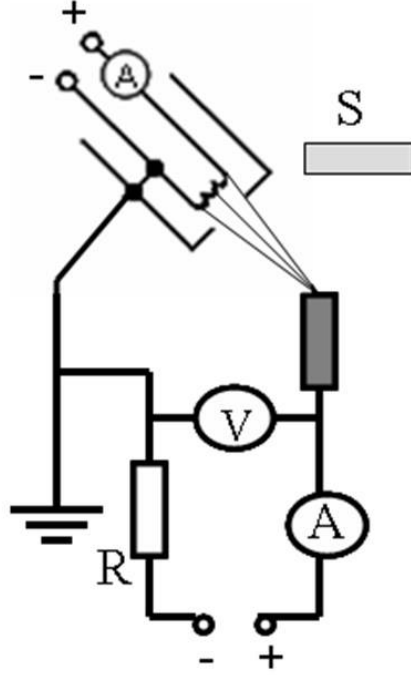


Figure 1: Experimental set-up of TVA plasma for tungsten layer deposition, S represents the substrates.

The anode temperature was used for estimation of the vapor pressure  $P_v$  and subsequently the speed of evaporation (the number of evaporated species per second) using relations (2) and (3),

$$\log P = A - \frac{B}{T} \quad (2)$$

$$\log N = \log (S \cdot P) + 22.546 - \log \sqrt{M \cdot T} \quad (3)$$

where  $A$  and  $B$  are given constants [7] which depend on the nature of material,  $M$  is the atomic mass of tungsten and  $S$  is the emitted surface of the anode. The vapor pressure needed for arc ignition in our deposition conditions is between  $2-10\text{ torr}$ , Figure 3. During plasma operation the vapor pressure has almost a constant value, practically the same value for both filaments currents.

Figure 4 shows the variation of evaporation rate with arc discharge obtained using relation [3]. It can be observed that the evaporation rate has constant value increasing with the arc discharge at a value of  $1 \cdot 10^{20} \text{ atoms/s}$ .

In the above mentioned TVA conditions the tungsten layer on stainless steel was obtained.

The AFM image of a tungsten layer is shown in Figure 5. As can be observed in this figure, the film is smooth, free cracks, homogenous, compact with a roughness of about  $5\text{ nm}$ .

Figure 6 shows the XRD patterns of the W layer. The results show that the W film has a cubic structure and the lattice constant:  $a = 0.316\text{ nm}$ . The diffraction intensity of

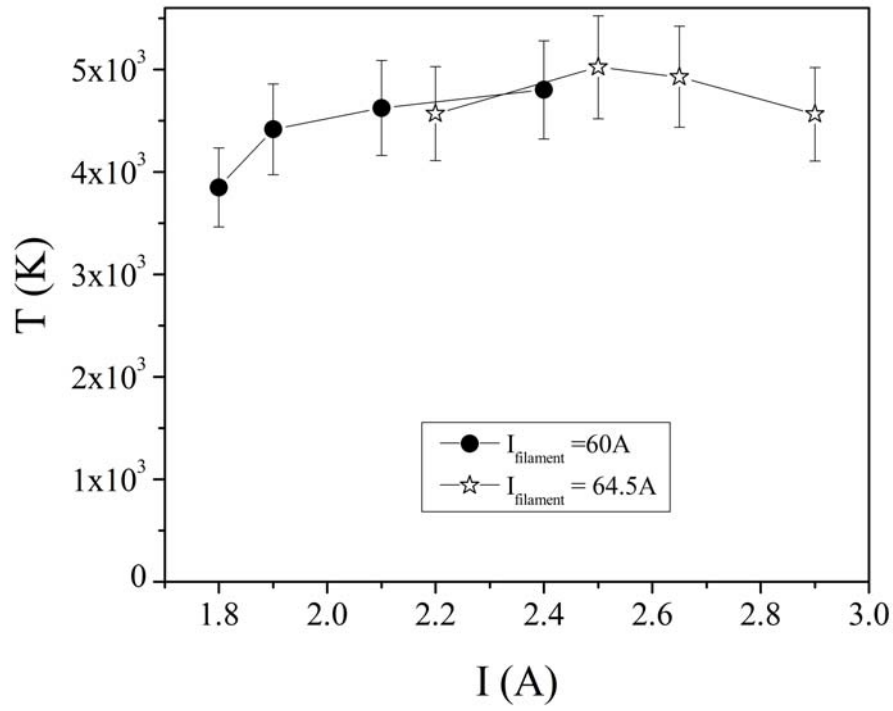


Figure 2: Variation of the top anode temperatures during deposition process versus arc discharge current.

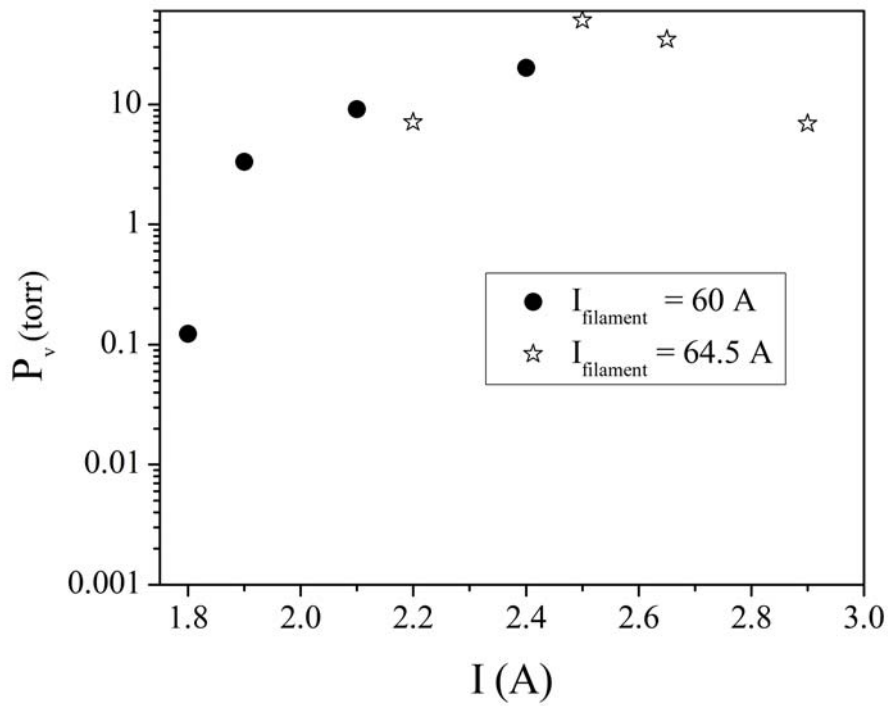


Figure 3: The variation of the vapor pressure during TVA discharge versus arc current.

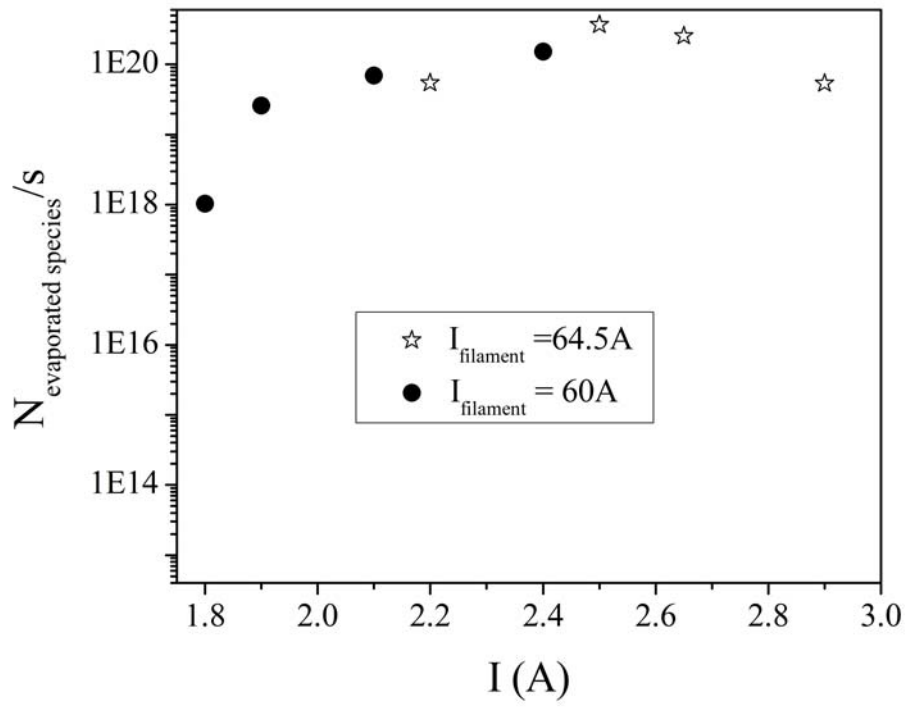


Figure 4: The evaporated speed during the TVA discharges for two filaments currents versus arc discharge.

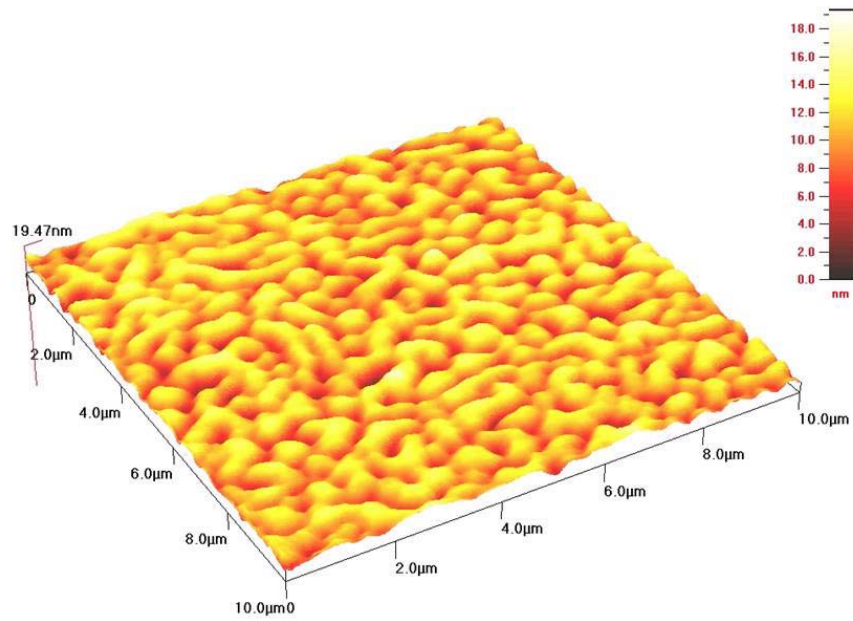


Figure 5: The AFM image on the tungsten layer deposited on a stainless steel. The roughness is 5 nm.

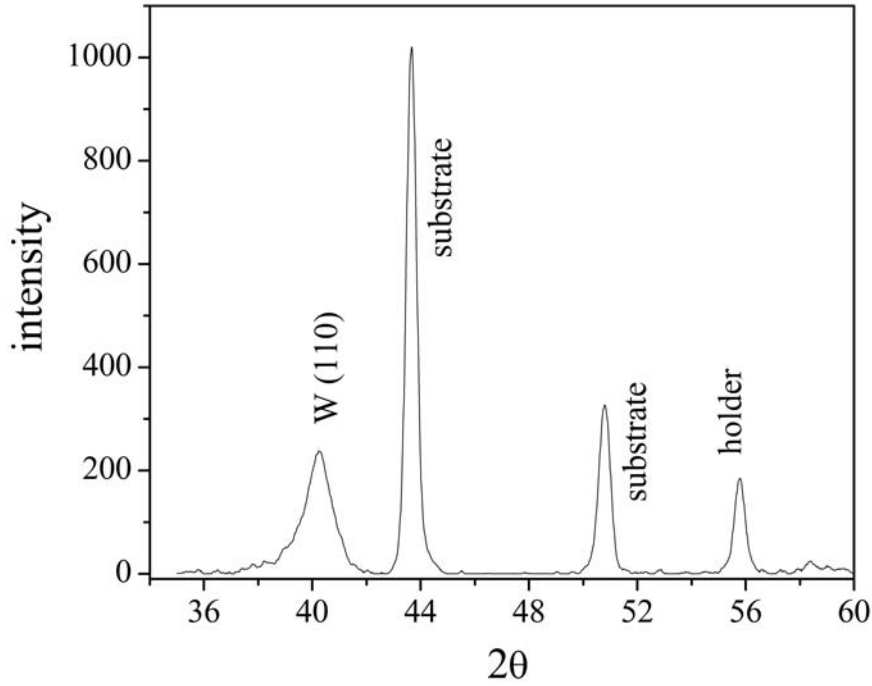


Figure 6: The XRD spectrum of the tungsten layer deposited on stainless steel substrate.

(110) is the strongest, when  $2\theta = 40^\circ$ .

Ignoring the microstraining effect (which affects the XRD peak width), as a first-order approximation, the average crystalline size can be estimated by the Debye – Scherrer formula [9],[10]:

$$D = \frac{K\lambda}{\beta \cos \theta} \quad (4)$$

where  $\lambda$  is the wavelength of X-ray used ( $CuK\alpha = 1,5421\text{\AA}$ ),  $\theta$  is the Bragg's angle (in radian),  $K$  is the shape factor of the particle (0.89, assuming that we have circular grains in our probes), and  $\beta_{1/2}$  is the full width at half-maximum (FWHM).

It is observed that the average particle size for tungsten deposited on stainless steel substrates, lies in the range of  $6 - 8nm$ .

## 4 Conclusion

The plasma TVA parameters as anode temperature, vapor pressure and evaporation speed were obtained in plasma stable conditions for two filaments currents. The plasma parameters were found to be almost the same for those values of the filament currents. It was observed that during deposition the plasma parameters had constant values.

The surface of W film is comparatively compact and smooth. The W film has a body-centered cubic structure, the lattice constant:  $a = 0.316nm$ , the growth preferred orientations of the film are (110). The roughness of the tungsten layer was  $5nm$  shown

that the film is quite smooth and compact. The average particles size calculated by Scherrer's formula lies in the range of  $6 - 8nm$ .

## References

- [1] S. Goulart-Santos, C. Godoy, M.M.R. Castro, International Journal of Refractory Metals & Hard Materials 26, 555–562 (2008).
- [2] Zhu Li-Na, Li Guo-Lu , Wang Hai-Dou , Xu Bin-Shi, Zhuang Da-Ming, Liu Jia-Jun, Current Applied Physics, 9, 510-514 (2009).
- [3] A.A. Joraid, Current Applied Physics, 9, 73-79 (2009).
- [4] C.S. Blackman, X. Correig, V. Katko, A. Mozalev, I.P. Parkin, R. Alcubilla, T. Trifonov, Materials Letters, 62, 4582-4584 (2008).
- [5] C.C. Surdu Bob, C.P. Lungu, I. Mustata and L. Frunza, J. Phys. D: Appl. Phys. 41, 132001, (2008).
- [6] V. Kuncser, I. Mustata, C.P. Lungu, A.M. Lungu, V. Zaroschi, W. Keune, B. Sahoo, F. Stromberg, M. Walterfang, L. Ion and G. Filoti, Surf. Coat. Technol. 200, 980–983 (2005).
- [7] A. Roth, Vacuum Technology, Elsevier, 1976.
- [8] M. Osiac, C.C. Surdu-Bob, C. Iacob and C.P. Lungu, Proc. 18th ISPC (Kyoto, Japan) p 121 (2007).
- [9] H. Klug, L. Alexander, X-ray diffraction procedures, John Wiley and Sons, Inc., New York, 491, 1962.
- [10] B. D. Cullity, Elements of X-ray Diffraction, Addison- Wesley, Reading, MA, 1978.